Surface morphology and transport studies of epitaxial graphene on SiC(0001[over_])

G. L. Creeth, A. J. Strudwick, J. T. Sadowski, and C. H. Marrows

Phys. Rev. B **83**, 195440 — Published 31 May 2011

DOI: 10.1103/PhysRevB.83.195440

Surface morphology and transport studies of epitaxial graphene on SiC ($000\bar{1}$)

G. L. Creeth,[1,*] A. J. Strudwick,[1] J. T. Sadowski,[2] and C. H.Marrows[1,†]

[1]*School of Physics & Astronomy, University of Leeds, Leeds LS2 9JT, United Kingdom*
[2]*Center for Functional Nanomaterials, Brookhaven National Laboratory, Upton, New York 11973, USA*

(Dated: April 20, 2011)

Annealing conditions are critical to the properties of epitaxial graphene formed by thermal decomposition of silicon carbide. Here we report the evolution of coherent electronic transport with increasing anneal temperatures, combined with low energy electron micrographs of equivalent surfaces showing corresponding structural coherence. Ultrahigh vacuum conditions and temperatures in the range of 1250°C to 1300°C produce granular films with a lateral grain size of approximately 20 nm, while temperatures of 1400°C or higher result in grains with progressively larger lateral dimensions in the micron range. Transport measurements show how the electronic coherence length increases as a result of the more coherent physical structure, with a crossover from two-dimensional variable range hopping to the weak localization regime. Here we show that whilst the duration of the anneal affects coverage and clustering of grains, the size of individual grains is determined by anneal temperature, with evidence of coalescence of smaller grains into larger domains, suggesting that multi-stage anneals at different temperatures may yield high-quality graphene.

PACS numbers: 71.23.An, 73.20.Fz, 73.22.Pr, 73.63.Bd

I. INTRODUCTION

Silicon carbide is a promising starting material for the production of large-scale areas of graphene,[1,2] a single atomic layer of carbon with remarkable properties.[3] While the technique of micromechanical cleavage, which was initially used to produce graphene,[4] yields high-quality material capable of exhibiting all of graphene's extraordinary behavior,[5,6] larger-scale devices and applications require the lateral dimensions of the material to be increased to the wafer scale. One way that this can be done is growth of so-called epitaxial graphene on commercial SiC wafers, which can be achieved by simply heating the substrate under appropriate conditions,[7] a fact actually known for decades.[8] The silicon present in the SiC structure has a lower vapor pressure than, and evaporates preferentially to, the carbon, leaving a carbon-rich region which can then form a surface layer of few or monolayer graphene.[9]

The electronic properties of graphene motivate the research field,[10] yet these can be only partially ascertained by many of the surface science techniques generally employed to study epitaxial graphene. While it is possible to show that a region of the material displays desirable properties in terms of structure and atomic register with respect to the substrate,[11] or band structure,[12] these measurements are made only over a very small area, or show an average over a larger area. Drawing conclusions regarding optimal growth conditions based on these techniques is therefore problematic, as electrical measurements[13,14] probe the system over a larger area while giving a less forgiving view of the quality of the film than an averaged measurement.

Here we show the connection between surface morphology (using low-energy electron microscopy (LEEM) and atomic force microscopy (AFM)) and transport data from devices of an equivalent size to the typical LEEM field-of-view (5 or 10 μm was used in this experiment), for samples grown under various conditions, linking transport regimes and electronic coherence to the characteristics of the surface layer. LEEM has been shown to be capable of determining the number of different layers in an epitaxial graphene film making use of the quantized oscillation in the electron reflectivity spectra obtained as function of start voltage in the microscope.[15] As well as being used to demonstrate large graphene terraces in the recent work of Emtsev et al.,[14] the LEEM technique has been used to study growth on the (0001) surface as a function of temperature,[16] the effects of substrate mis-orientation on 6H material,[17] and to discriminate between AB and AC stacking in bilayer epitaxial graphene.[18] LEEM therefore offers the possibility of characterizing graphene over a length-scale equal to the separation between contacts defined by optical lithography for transport measurements, and with sufficient sensitivity to detect to defects involved in modifications to the electron transport.

II. METHODS

Graphitization was carried out on substrate SiC wafer sections measuring 5 mm × 10 mm (semi-insulating 4H SiC in order to facilitate transport measurements) by annealing at various temperatures under UHV conditions (base pressure $< 10^{-10}$ mbar). This produced graphene on both (0001) and ($000\bar{1}$) faces, although the carbon-terminated

$(000\overline{1})$ face was used for all measurements presented here, motivated by the retention of monolayer properties for multilayer systems[19]. The temperature was measured by using a thermocouple on the sample manipulator that was previously calibrated using optical pyrometry. Following the anneal, the samples were probed using *in-situ* low-energy electron diffraction (LEED). LEED patterns taken after the growth of the samples discussed below are not shown: all exhibited the typical dashed ring pattern for C-face material indicating graphene growth with preferred orientations and a background of more general rotational disorder[19]: samples that we shall see have very different morphologies and transport properties are not easily distinguishable on the basis of LEED alone.

The samples were then characterized *ex-situ*. Raman spectroscopy (also not shown) confirmed the presence of graphene-like peaks[20] on a SiC background,[21,22] again all had similar spectra. Atomic force microscopy was used to determine surface morphology, whilst an Elmitec LEEM V was used to probe the near-surface graphene structure. Intensity-voltage measurements in real space (IV LEEM) have been used to determine the thicknesses of graphene domains, their sizes, and distribution on the substrate. Transport data presented here are dc measurements of sheet material carried in a constant-flow cryostat, using a 4-probe technique with a voltage-probe separation of 5 μm, with the Ti/Au probes prepared using standard optical lithography methods.

III. RESULTS

A. Lateral grain size

As described above, LEEM is a powerful technique for investigating epitaxial graphene. In Fig. 1 we show LEEM images for samples annealed under various conditions. A short 20 minute anneal at 1300°C resulted in a graphene-like LEED pattern (not shown), but no significant graphene on the surface was found in the image [Fig. 1(a)], while a longer one hour anneal at that temperature forms an appreciable surface covering of graphene, indicated by the darker features visible in Fig. 1(b). The difference in coverage can be attributed to the silicon depletion process continuing for longer. In both cases some non-uniformity can be seen to follow macroscopic deformities (polishing scratches) and may also depend on smaller localized defects, with clusters of grains following these local features.

Annealing at a higher temperature of 1400°C results in a higher coverage and a noticeably larger lateral grain size, as can be seen in the micrographs of samples annealed for 30 minutes [Fig. 1(c)] and 55 minutes [Fig. 1(d)] at that temperature. The coverage is more uniform, with no observed correlation to surface defects. Graphene domains are larger and more angular in shape, and longer durations at this temperature do not result in significant changes to the surface, although a slight increase in uniformity can perhaps be discerned.

AFM is useful for investigating these surfaces at finer lengthscales, enabling a distinction to be made between clustering into domains and coalescence (or 'coarsening'[23]). From the LEEM image in Fig. 1(b) there appear to be features giving contrast on the micron scale; AFM of this surface shows that within these clusters the individual grains measure only ~ 20 nm in diameter [Fig. 2(a)]. In marked contrast, for the sample annealed at the higher temperature of 1400°C [as in the LEEM image in Fig. 1(c)], AFM shows domains with faceted edges [Fig. 2(b)], and not clusters of grains, essentially reproducing the same features seen in the LEEM image. Candidate growth mechanisms that would give rise to such contrasting surfaces are individual grains propagating faster at higher temperatures or coalescence of small grains into larger ones. The mechanisms are not mutually exclusive, and it is difficult to definitively assign our results to either of them on the basis of these data alone.

In order to differentiate between these two mechanisms, a sample was annealed under standard conditions at 1300°C, followed by an additional anneal at 1400°C for 30 minutes. AFM of the surface revealed faceted graphene domains [Fig. 2(c)] resembling those for samples which underwent a single high-temperature anneal [as in Fig. 2(b)]. As the uppermost graphene layer is the first to be grown,[24] this gives a clear indication that grains are able to coalesce, with carbon atoms mobile enough for boundaries to be erased during the anneal; we shall see below that the transport properties for this sample corroborate this increased lateral scale.

Samples annealed at still higher temperatures continue the trend towards larger domain sizes. Fig. 1(e) shows a 5 μm field-of-view LEEM image within which large regions of uniform-looking graphene can be seen, with some extending across the whole width of the image. AFM confirms the smoother, laterally more coherent structure of the graphene surface for this sample [Fig. 2(d)].

IV LEEM can be used to be used to identify how many layers of graphene are present,[15,23] and we find each of these large areas to be of a particular thickness. Fig. 1(f) shows IV-LEEM data for the sample annealed at 1450°C. The number of minima in the signal corresponds to the number of graphene monolayers present at each marked point in Fig. 1(e). We can hence see that within the field of view there are two large areas of bilayer and trilayer graphene respectively, together with a smaller area consisting of four layers. These are quite low thicknesses for the SiC $(000\overline{1})$ face, where rather thick multilayers are usually found (see, for instance, Ref. 19). Similar analysis shows that all of the samples considered here are of comparable thickness, that is typically three monolayers thick with about one layer

of variation from this mean. The fact that the Raman spectra show no significant variation in the attenuation of the SiC substrate signal supports this conclusion.

In the absence of significant thickness variation, it is the samples' morphology, as seen in the LEEM images and AFM micrographs, that can be expected determine the transport properties of the various graphene epilayers studied here. We now turn to low-temperature measurements where we probe these effects.

IV. TRANSPORT MEASUREMENTS

The transport mechanisms of materials are often revealed by the temperature dependence of the resistivity ρ.[25] In thin films, a convenient measure of this quantity is the sheet resistance $R_{\rm s}$. In Fig. 3 we present $R_{\rm s}(T)$ data for samples annealed as described previously, which all become monotonically more resistive as they are cooled from room temperature. For all samples annealed at 1300°C, $R_{\rm s}(T)$ above ~ 5 K is well described by a variable range hopping (VRH) behavior, given by[26]

$$R_{\rm s}(T) = R_0 \exp\left(\frac{T_0}{T}\right)^{\frac{1}{n+1}}, \tag{1}$$

where n is the dimensionality of the system. The data shown in Fig. 3 can be seen to be consistent with a $\ln R_{\rm s} \sim T^{-1/3}$ law, appropriate to 2-dimensional VRH. This may be understood in terms of the system being studied: any few atomic layers of conductive material on an insulating surface should exhibit 2D behavior, while the grain size from AFM indicates a high degree of disorder leading to VRH. (This description was also used for the near insulating behavior of graphane (hydrogenated graphene),[27] or bilayer graphene with a discontinuous top-gate dielectric layer,[28] both instances where a gap is opened up in random locations in the graphene sheet.)

Some samples (those annealed for shorter durations) are effectively insulating at temperatures below ~ 30 K, while a longer anneal leads to a surface which conducts down to the lowest temperatures attainable in the cryostat (~ 1.3 K). In all cases the change in resistance with temperature indicates a strongly non-metallic regime, with an increase in resistance over orders of magnitude between room and helium temperature. The samples' activation energies take two distinct values, $\sim$ 7-10 eV for the short anneals, $\sim$ 2-8 meV for the longer ones. The former energy scale is so large that it must correspond to tunneling between discontinuous grains that are not in electronic contact, whilst the latter represents clustered granular material (see Fig 1(a) and 1(b) respectively). While the epitaxial nature of the graphene is indicated by the LEED data showing preferred angular orientations, the long-range order is not sufficient for the electronic transport to be graphene-like.

Although the samples annealed at 1400°C (or higher) were also found to become less conducting as they are cooled, the $R_{\rm s}(T)$ data cannot be fitted to this functional form. For these samples the larger continuous areas of graphene allow a longer electronic mean free path ℓ, the product of which with the Fermi wavevector $k_{\rm F}$ now exceeds unity. The increased structural coherence results in less frequent inelastic scattering and elastic collisions dominate, increasing the possibility of electrons tracing a closed path while remaining phase-coherent and leading to weak localization (WL).[29] The correction to the conductance G in the WL regime is given by

$$G = \left(\frac{ne^2\tau_0}{m}\right)\left[1 - \frac{1}{\pi k_{\rm F}\ell}\ln\left(\frac{\tau_{\rm i}}{\tau_0}\right)\right]. \tag{2}$$

As τ_0, the elastic scattering time, is not temperature dependent, the temperature dependence is a result of $\tau_{\rm i}$, the inelastic scattering time, and overall the change in resistance is proportional to $\ln T$,[29] as seen previously for epitaxial graphene.[7] In Fig. 3(b) we show data for three such samples. The sample annealed at 1450°C was roughly two orders of magnitude more conducting than those annealed at 1400 °C (and so the data are scaled by $\times 100$ in order to be displayed on the same plot). The coalescence observed using AFM for the sample initially annealed at 1300°C results in an accompanying increase in electron inelastic scattering lifetime. For samples annealed at 1300°C, a change in electronic behavior can be discerned below 5 K; the data no longer follow Eq. 1 and do instead show a reasonable linear relationship when plotted as $\ln R_{\rm s}$ vs. T as in Fig. 3(b).

It is instructive to compare our results with those found in the past on other carbon-based systems where $\rho(T)$ has been measured. There is a general trend in conduction type from VRH to WL as disorder is reduced. Electrospun pregraphitic carbon fiber is highly disordered, with $k_{\rm F}\ell \sim 1$, and so strongly localized: such material showed a VRH behavior,[30] although of the Efros-Shklovskii type.[31] Individual monolayers of chemically derived graphene were also found to be sufficiently disordered to show clear two-dimensional VRH.[32]Plasma-deposited amorphous carbon films showed a crossover from VRH to WL as the temperature is varied.[33] Various forms of bulk graphite were studied by Koike et al., who found the signature of WL in poorly-ordered ($\rho \sim 10^{-3}$ Ωcm) Ceylon graphite and Grafoil, but

metallic behavior in well-ordered ($\rho \sim 10^{-5}$ Ωcm) highly-oriented pyrolytic graphite (HOPG) and single crystal Kish graphite.[34] We can see that the best of our samples are approaching the more ordered end of this spectrum, but are still not so perfect as the HOPG or Kish graphite.

V. CONCLUSIONS

Interest in graphene as a material and the search for techniques enabling large areas to be fabricated are motivated by graphene's extraordinary electronic transport properties. For UHV-grown material in this study, LEED data indicated epitaxial growth but was not able to distinguish between samples that went on to show very different transport properties at cryogenic temperatures. While LEED indicates the onset of graphene growth, AFM can measure grain dimensions at small length-scales, while the continuity of the granular surface over a longer length scale is critical for transport. Assessments of this continuity as inferred from transport properties and as imaged via LEEM are seen to be complementary, and to support a model of growth processes for granular graphene films involving clustering of granular material, and coalescence of grains combined with significantly increased mobility of surface carbon at higher temperatures. Taking our results in the round, we observe four stages of graphene growth: short anneals at 1300°C or less give discontinuous grains and insulating behavior at helium temperature; longer anneals at this temperature give 2-dimensional VRH to much lower temperatures with the energy scale reduced from eV to meV; anneals at 1400°C give continuous terraces of few-layer graphene and a cross-over to the WL regime; anneals at 1450°C give smoother morphology still, with WL and a reduction of sheet resistance to < 100 $\Omega/\Box$ over the entire measured temperature range.

Acknowledgments

The authors acknowledge financial support from the United Kingdom EPSRC and Intel Ireland. Research carried out (in whole or in part) at the Center for Functional Nanomaterials, Brookhaven National Laboratory, which is supported by the U.S. Department of Energy, Office of Basic Energy Sciences, under Contract No. DE-AC02-98CH10886.

* Electronic address: g.l.creeth@leeds.ac.uk
† Electronic address: c.h.marrows@leeds.ac.uk

[1] T. Seyller, A. Bostwick, K. V. Emtsev, K. Horn, L. Ley, J. L. McChesney, T. Ohta, J. D. Riley, E. Rotenberg, and F. Speck, Phys. Stat. Sol. (b) **245**, 1436 (2008).
[2] W. A. de Heer, C. Berger, X. Wu, M. Sprinkle, Y. Hu, M. Ruan, J. A. Stroscio, P. N. First, R. Haddon, B. Piot, et al., J. Phys. D: Appl. Phys. **43**, 374007 (2010).
[3] A. K. Geim and K. S. Novoselov, Nature Materials **6**, 183 (2007).
[4] K. S. Novoselov, D. Jiang, F. Schedin, T. J. Booth, V. V. K. andS. V. Morozov, and A. K. Geim, Proc. Nat. Acad. Sci. **102**, 10451 (2005).
[5] K. S. Novoselov, A. K. Geim, S. V. Morozov, D. Jiang, M. I. Katsnelson, I. V. Grigorieva, S. V. Dubonos, and A. A. Firsov, Nature (London) **438**, 197 (2005).
[6] Y. B. Zhang, Y. W. Tan, H. L. Stormer, and P. Kim, Nature (London) **438**, 201 (2005).
[7] C. Berger, Z. Song, T. Li, X. Li, A. Ogbazghi, R. Feng, Z. Dai, A. Marchenkov, E. Conrad, P. First, et al., J. Phys. Chem. B **108**, 19912 (2004).
[8] A. Van Bommel, J. Crombeen, and A. Van Tooren, Surf. Sci. **48**, 463 (1974).
[9] A. Charrier, A. Coati, T. Argunova, F. Thibaudau, Y. Garreau, R. Pinchaux, I. Forbeaux, J.-M. Debever, M. Sauvage-Simkin, and J.-M. Themlin, J. Appl. Phys. **92**, 2479 (2002).
[10] A. H. Castro Neto, F. Guinea, N. M. R. Peres, K. S. Novoselov, and A. K. Geim, Rev. Mod. Phys. **81**, 109 (2009).
[11] F. Varchon, P. Mallet, J.-Y. Veuillen, and L. Magaud, Phys. Rev. B **77**, 235412 (2008).
[12] A. Bostwick, T. Ohta, T. Seyller, K. Horn, and E. Rotenberg, Nature Physics **3**, 36 (2007).
[13] C. Berger, Z. Song, X. Li, X. Wu, N. Brown, C. Naud, D. Mayou, T. Li, J. Hass, A. N. Marchenkov, et al., Science **312**, 1191 (2006).
[14] K. V. Emtsev, A. Bostwick, K. Horn, J. Jobst, G. L. Kellogg, L. Ley, J. L. McChesney, T. Ohta, S. A. Reshanov, J. Rohrl, et al., Nature Materials **8**, 203 (2009), ISSN 1476-4660.
[15] H. Hibino, H. Kageshima, F. Maeda, M. Nagase, Y. Kobayashi, and H. Yamaguchi, Phys. Rev. B **77**, 075413 (2008).
[16] T. Ohta, F. El Gabaly, A. Bostwick, J. L. McChesney, K. V. Emtsev, A. K. Schmid, T. Seyller, K. Horn, and E. Rotenberg, New J. Phys. **10**, 023034 (2008).
[17] C. Virojanadara, R. Yakimova, J. Osiecki, M. Syvjrvi, R. Uhrberg, L. Johansson, and A. Zakharov, Surf. Sci. **603**, L87 (2009).
[18] H. Hibino, S. Mizuno, H. Kageshima, M. Nagase, and H. Yamaguchi, Phys. Rev. B **80**, 085406 (2009).
[19] J. Hass, F. Varchon, J. E. Millan-Otoya, M. Sprinkle, N. Sharma, W. A. de Heer, C. Berger, P. N. First, L. Magaud, and E. H. Conrad, Phys. Rev. Lett. **100**, 125504 (2008).
[20] A. C. Ferrari, J. C. Meyer, V. Scardaci, C. Casiraghi, M. Lazzeri, F. Mauri, S. Piscanec, D. Jiang, K. S. Novoselov, S. Roth, et al., Phys. Rev. Lett. **97**, 187401 (pages 4) (2006).
[21] J. Rohrl, M. Hundhausen, K. V. Emtsev, T. Seyller, R. Graupner, and L. Ley, Appl. Phys. Lett. **92**, 201918 (2008).
[22] A. J. Strudwick, G. L. Creeth, N. A. B. Johansson, and C. H. Marrows, Appl. Phys. Lett. **98**, 051910 (2011).
[23] Luxmi, N. Srivastava, G. He, R. M. Feenstra, and P. J. Fisher, Phys. Rev. B **82**, 235406 (2010).
[24] K. V. Emtsev, F. Speck, T. Seyller, L. Ley, and J. D. Riley, Phys. Rev. B **77**, 155303 (2008).
[25] P. L. Rossiter, *The Electrical Resistivity of Metals and Alloys* (Cambridge University Press, Cambridge, 1987).
[26] N. F. Mott, Phil. Mag. **19**, 835 (1969).
[27] D. C. Elias, R. R. Nair, T. M. G. Mohiuddin, S. V. Morozov, P. Blake, M. P. Halsall, A. C. Ferrari, D. W. Boukhvalov, M. I. Katsnelson, A. K. Geim, et al., Science **323**, 610 (2008).
[28] S. Russo, M. F. Craciun, M. Yamamoto, S. Tarucha, and A. F. Morpurgo, New J. Phys. **11**, 095018 (2009).
[29] G. Bergmann, Phys. Rev. B **28**, 2914 (1983).
[30] Y. Wang and J. J. Santiago-Avilés, Appl. Phys. Lett. **89**, 123119 (2006).
[31] A. L. Efros and B. I. Shklovskii, J. Phys. C **8**, L49 (1975).
[32] A. B. Kaiser, C. Gómez-Navarro, R. S. Sundaram, M. Burghard, and K. Kern, Nano Letters **9**, 1787 (2009).
[33] S. Bhattacharyya, Appl. Phys. Lett. **91**, 142116 (2007).
[34] Y. Koike, S. Morita, T. Nakamonyo, and T. Fukase, J. Phys. Soc. Japan **54**, 713 (1985).

Figures

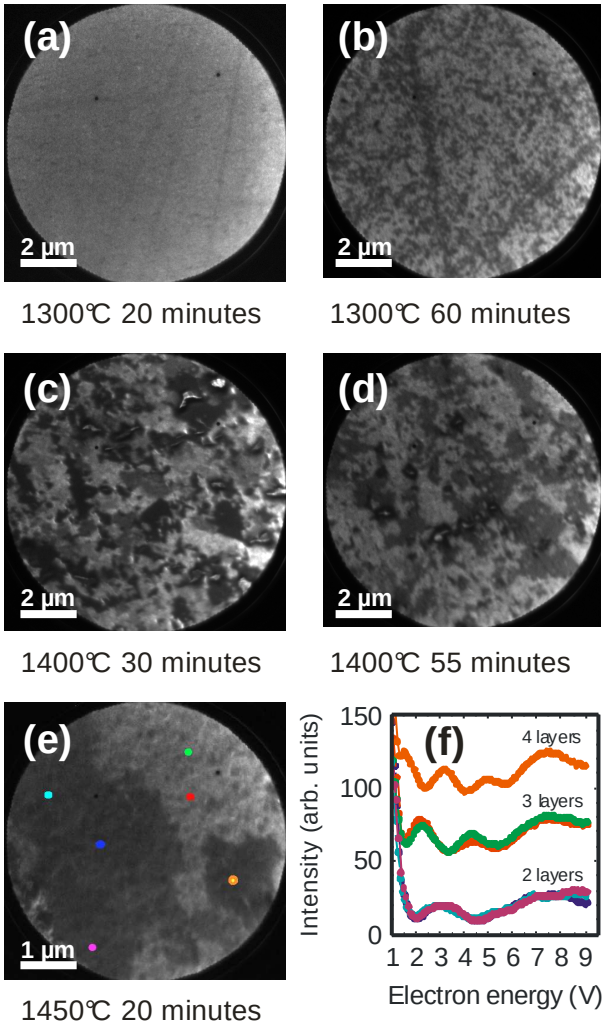

FIG. 1: (Color online) LEEM studies. (a)-(e) LEEM images of the graphitized $(000\bar{1})$ face of 4H SiC, annealed under the conditions indicated in each panel. All images were acquired at an incident electron energy of 4.5 eV. Note the different scale bar for image (e). (f) Local IV LEEM data for the sample shown in panel (e), with the various curves taken at the spots marked in that image. The curves are offset for clarity. The number of minima in the curves show that the large dark region on the left of (e) is bilayer graphene, the light region in the center is trilayer graphene, and the small dark region on the right is quadruple-layer material.

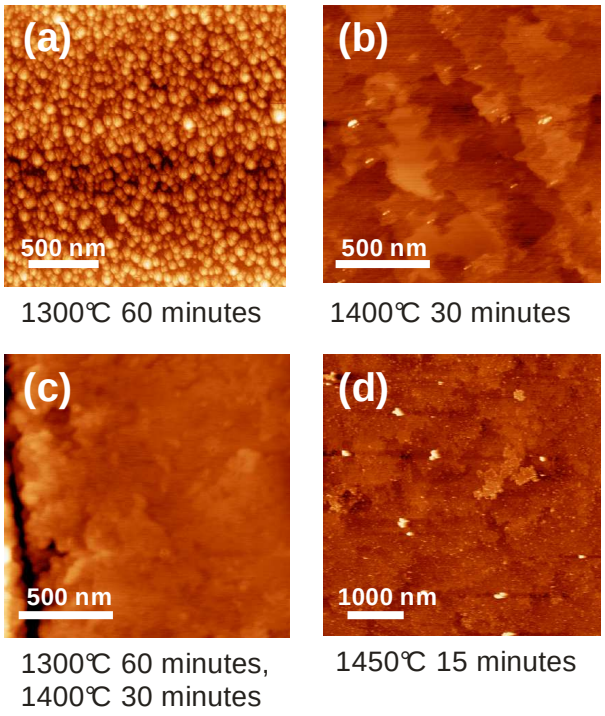

FIG. 2: (Color online) AFM images of graphitized samples, for anneal conditions of (a) 60 minutes at 1300°C, (b) 30 minutes at 1400°C, (c) 60 minutes 1300°C followed by 30 minutes at 1400°C, and (d) 15 minutes at 1450°C. Note the variation in lateral scale between the images. The samples shown in (a) and (b) are the same two samples shown in Fig. 1(b) and (c). The full range of the height scale in panel (a) is 20 nm, in panels (b) and (c) it is 6 nm, and in (d) it is 4 nm. A small amount of additional debris is visible on the surface of this last sample giving rise to some bright speckles in the image.

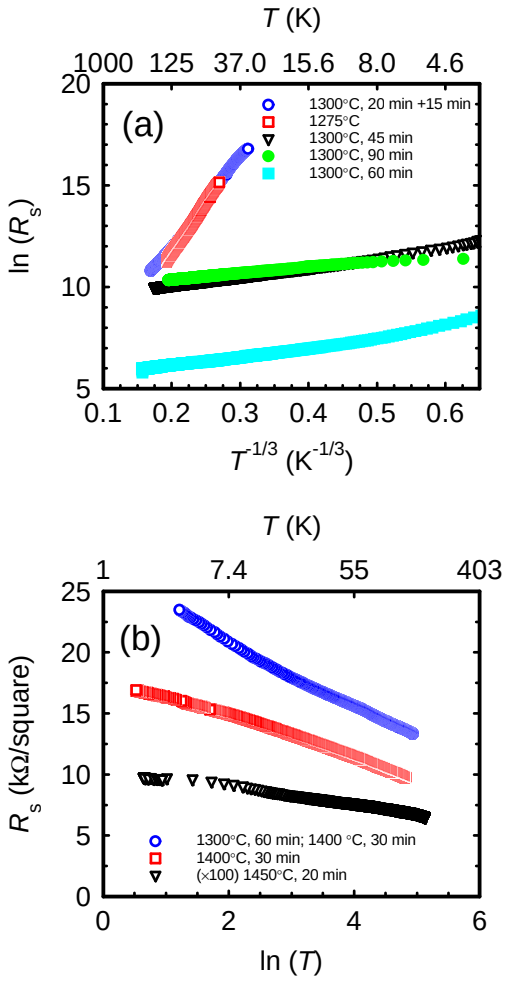

FIG. 3: (Color online) Resistance change with temperature for samples annealed at a variety of temperatures and durations. (a) Data for samples annealed at 1300°C and below, plotted on appropriate axes for a 2-dimensional VRH-type behavior. The most resistive samples become so poorly conducting at low T that they are unmeasurable. (b) Data for samples annealed at 1400°C and above, plotted on appropriate axes for a WL-type behavior. Note that the data for the sample annealed at 1450°C have been scaled up by a factor of 100 in sheet resistance for visibility, due to the very high conductivity of this sample.